

Neurophysiologic Correlates of Ketamine Sedation and Anesthesia

A High-density Electroencephalography Study in Healthy Volunteers

Phillip E. Vlisides, M.D., Tarik Bel-Bahar, Ph.D., UnCheol Lee, Ph.D., Duan Li, Ph.D., Hyoungkyu Kim, Ph.D., Ellen Janke, M.D., Vijay Tarnal, M.D., Adrian B. Pichurko, M.D., Amy M. McKinney, M.A., Bryan S. Kunkler, M.D., M.S., Paul Picton, M.B. Ch.B., M.R.C.P., F.R.C.A., George A. Mashour, M.D., Ph.D.

ABSTRACT

Background: Previous studies have demonstrated inconsistent neurophysiologic effects of ketamine, although discrepant findings might relate to differences in doses studied, brain regions analyzed, coadministration of other anesthetic medications, and resolution of the electroencephalograph. The objective of this study was to characterize the dose-dependent effects of ketamine on cortical oscillations and functional connectivity.

Methods: Ten healthy human volunteers were recruited for study participation. The data were recorded using a 128-channel electroencephalograph during baseline consciousness, subanesthetic dosing (0.5 mg/kg over 40 min), anesthetic dosing (1.5 mg/kg bolus), and recovery. No other sedative or anesthetic medications were administered. Spectrograms, topomaps, and functional connectivity (weighted and directed phase lag index) were computed and analyzed.

Results: Frontal theta bandwidth power increased most dramatically during ketamine anesthesia (mean power \pm SD, 4.25 ± 1.90 dB) compared to the baseline (0.64 ± 0.28 dB), subanesthetic (0.60 ± 0.30 dB), and recovery (0.68 ± 0.41 dB) states; $P < 0.001$. Gamma power also increased during ketamine anesthesia. Weighted phase lag index demonstrated theta phase locking within anterior regions (0.2349 ± 0.1170 , $P < 0.001$) and between anterior and posterior regions (0.2159 ± 0.1538 , $P < 0.01$) during ketamine anesthesia. Alpha power gradually decreased with subanesthetic ketamine, and anterior-to-posterior directed connectivity was maximally reduced (0.0282 ± 0.0772) during ketamine anesthesia compared to all other states ($P < 0.05$).

Conclusions: Ketamine anesthesia correlates most clearly with distinct changes in the theta bandwidth, including increased power and functional connectivity. Anterior-to-posterior connectivity in the alpha bandwidth becomes maximally depressed with anesthetic ketamine administration, suggesting a dose-dependent effect. (**ANESTHESIOLOGY 2017; 127:58-69**)

KETAMINE is a general anesthetic with unique features at the molecular, neural, and behavioral levels. Unlike the intravenous and inhaled anesthetics in common clinical use, ketamine is thought to work primarily by antagonizing *N*-methyl-D-aspartate (NMDA) receptors¹⁻⁴ and hyperpolarization-activated, cyclic-nucleotide-gated channel 1,^{5,6} without strong agonist effects on synaptic γ -aminobutyric acid (GABA) receptors. Furthermore, electroencephalographic characteristics of ketamine anesthesia are distinct from those associated with anesthetics that act primarily *via* GABA-receptor agonism. For example, coherent frontal alpha oscillations are observed with propofol-induced unconsciousness^{7,8} that are believed to result from thalamocortical hypersynchrony⁹ and that possibly inhibit corticocortical communication.⁸ These same patterns are noted with ether-based volatile anesthetics during surgical

What We Already Know about This Topic

- Ketamine is a unique anesthetic with neural effects that are distinct from more commonly-used γ -aminobutyric acid agonists
- Although various electroencephalography studies of ketamine have been performed, none have assessed spectral power and connectivity at subanesthetic and anesthetic doses

What This Article Tells Us That Is New

- Ketamine had dose-dependent effects on spectral power, functional connectivity, and directed connectivity
- Anesthetic doses of ketamine resulted in markedly increased theta power across the cortex as well as increased gamma and delta power
- Increased anterior-posterior connectivity in the theta bandwidth and decreased connectivity in the alpha bandwidth were specific for ketamine anesthesia

This article is featured in "This Month in Anesthesiology," page 1A. P.E.V. and T.B.-B. contributed equally to this article. Supplemental Digital Content is available for this article. Direct URL citations appear in the printed text and are available in both the HTML and PDF versions of this article. Links to the digital files are provided in the HTML text of this article on the Journal's Web site (www.anesthesiology.org). This article has a video abstract.

Copyright © 2017, the American Society of Anesthesiologists, Inc. Wolters Kluwer Health, Inc. All Rights Reserved. Anesthesiology 2017; 127:58-69

levels of unconsciousness.¹⁰ Ketamine anesthesia, however, is not associated with these electroencephalographic characteristics.^{11,12} During anesthetic induction with ketamine, an increase in gamma power has been consistently reported,^{10,12,13} and when ketamine is administered in the presence of propofol or ether-based volatile anesthetics, there is a power shift to the beta bandwidth.^{14,15} These effects may be due to anti-NMDA-mediated disinhibition of pyramidal neurons¹⁶ and hyperpolarization-activated, cyclic-nucleotide-gated channel 1 inhibition.¹⁵

Previous studies^{11–13} have examined the electroencephalographic effects of ketamine, but the precise neurophysiologic correlates remain unclear for a number of reasons. For example, ketamine has often been studied in the presence of other concomitantly administered sedative and anesthetic medications,^{13,14,17} potentially altering or obfuscating neurophysiologic signatures specific to ketamine. Additionally, electroencephalogram studies to date have been constrained by either regionally limited analyses or low-resolution acquisition.^{11–13} Studies have also focused on either subanesthetic^{18,19} or anesthetic dosing,^{11–13} without being able to directly compare dose-dependent electroencephalographic characteristics. Last, there is a dearth of information regarding recovery from ketamine-induced anesthesia, as studies have tended to focus on the beginning of surgical cases, with GABAergic anesthetics often coadministered or administered directly after ketamine induction. Improving the understanding of ketamine-specific effects on the electroencephalogram may provide insights into the neuroscientific correlates of consciousness, particularly given the unique molecular, neural, and phenomenologic features of ketamine that differ from other anesthetics. Thus, in this study, we used spectral and connectivity analyses of high-density electroencephalographic recordings to characterize neurophysiologic changes associated with ketamine as a single agent during subanesthetic administration, anesthetic dosing, and a recovery period. We hypothesized that ketamine would induce distinct, dose-dependent effects on spectral and functional connectivity patterns that would distinguish between these arousal states.

Materials and Methods

This study was approved by the University of Michigan Medical School Institutional Review Board, Ann Arbor, Michigan (HUM00061087), and written informed consent was obtained from all participants before the study. All study procedures were conducted at the University of Michigan Medical School, Ann Arbor, Michigan. Ten volunteers were recruited from September 2015 through January 2016 using

recruitment flyers posted throughout the medical school and University Hospital of the University of Michigan, Ann Arbor, Michigan. Phone screening was conducted by a member of the research team to review inclusion and exclusion criteria before enrollment.

Study Population

Participants were considered eligible if they were American Society of Anesthesiologists physical status class I, between the ages of 20 and 40 yr, had a body mass index less than 30, and had no predictors of a difficult airway. Candidates were excluded from participation if they had cardiovascular disease, cardiac conduction abnormalities, hypertension, obstructive sleep apnea, asthma, ongoing respiratory illness, gastroesophageal reflux, history of drug use (or positive drug screen before the experiment), family history of problems with anesthesia, neurologic disorders, psychiatric disorders, or current pregnancy. The number of volunteers recruited was based on previous studies that investigated neurophysiologic correlates of anesthetic-induced unconsciousness.^{7,20}

Anesthetic Protocol

Experiments were conducted between the hours of 8:00 AM and 1:00 PM for all participants except for one (participant No. 2, studied between 4:00 PM and 7:00 PM). Before initiation of the experiment, a full medical and anesthetic history was obtained, and a physical examination was performed. All participants fasted from food and drink for 8 h before the experiment. Peripheral intravenous catheters were placed, and American Society of Anesthesiologists standard monitors were applied before drug administration. At least two anesthesiologists were present for the full duration of the experiment. All participants underwent the following stepwise protocol, with electroencephalogram data collection throughout each period:

1. a 5-min eye-closed resting period before ketamine administration (baseline condition)
2. subanesthetic ketamine infusion (0.5 mg/kg) over 40 min (subanesthetic condition) with eyes closed, followed by 8 mg ondansetron for nausea and vomiting prophylaxis
3. break for completion of questionnaire (data not reported here)
4. anesthetic (1.5 mg/kg) bolus dose (anesthetic condition) with eyes closed
5. recovery period (recovery condition) with eyes closed

Participants were instructed to keep their eyes closed throughout each of these recording periods. Rather than using target-controlled infusions, we chose dosing strategies that were directly relevant to clinical care for either depression (0.5 mg/kg over 40 min) or anesthetic induction (1.5 mg/kg bolus) to enhance the translational relevance of this study. Participants were monitored through both loss of consciousness

Submitted for publication November 13, 2016. Accepted for publication March 31, 2017. From the Department of Anesthesiology (P.E.V., T.B.-B., U.L., D.L., H.K., E.J., V.T., A.M.M., B.S.K., P.P., G.A.M.), Center for Consciousness Science (P.E.V., T.B.-B., U.L., D.L., H.K., G.A.M.), and Neuroscience Graduate Program (G.A.M.), University of Michigan Medical School, Ann Arbor, Michigan; and the Department of Anesthesiology, Northwestern University Feinberg School of Medicine, Chicago, Illinois (A.B.P.).

(LOC) and return of consciousness (ROC) using a previously described protocol²⁰; we acknowledge that our definition of LOC relates to consciousness of the environment and does not exclude the possibility of endogenous experiences such as dreams or hallucinations. In brief, volunteers held an object in each hand that makes a sound when squeezed. An audio loop then started playing that instructed participants, in a random manner, to squeeze their right or left hand. This audio loop would deliver a command every 30s, and the loop played before, during, and after anesthetic ketamine bolus administration. LOC was marked when subjects ceased to respond to two audio commands in a row. A scopolamine patch (1.5 mg) was also placed after ROC for further nausea and vomiting prophylaxis. Participants were then evaluated and monitored after the conclusion of the experiment. Additional antiemetics were administered if needed. Participants were discharged once they were awake, alert, and responsive; had no significant nausea or vomiting; were able to ambulate with minimal assistance; and had a responsible adult to accompany them home. Follow-up calls were made to patients both the evening after the experiment and the next day.

Electroencephalography Analysis

Data Acquisition. Electroencephalogram data were acquired with 128-channel HydroCel nets, Net Amps 400 amplifiers, and Net Station 4.5 software (Electrical Geodesics, Inc., USA). The electroencephalogram was digitized continuously at 500 Hz with a vertex reference. Per manufacturer recommendations, channel impedances were kept at less than 50 k Ω , and the net was wrapped with gauze to optimize contact between the electrodes and scalp.

Spectral Processing and Analysis. Data processing was performed with Chronux (<http://chronux.org/>)^{21,22} and custom MATLAB (MathWorks, USA) scripts and toolboxes. All visual inspection was performed by one of the investigators (T.B.-B.) trained in dense electroencephalography review. After each recording session, the data were bandpass-filtered at 0.5 to 55 Hz (eegiltnew, firfilt plugin, zero-phase, Hamming-windowed finite impulse response filter, 3,301 points (6.6s), 0.5 Hz transition band, 0.5 and 55 pass-band edges, -6 dB cutoff frequencies: 0.25 and 55.25) to decrease the influence of low-frequency drift and high-frequency artifacts. Electrodes on the lowest parts of the face and head were removed, leaving 98 remaining channels. Bad channels were then detected and removed using visual inspection and the *rejchan* and *clean rawdata* functions, with 86 to 91 channels retained. The channels were then average-referenced to the mean of the voltage across all remaining channels. Conditions of interest—the baseline eyes-closed period (5 min), subanesthetic infusion (0 to 38 min), anesthetic bolus dose (from LOC to 5 min after LOC, 3.8 min for one volunteer), and recovery period (5 min, collected 8 to 15 min after ROC)—were extracted from the data for each participant. These specific time epochs were chosen to include data relatively preserved from artifact and to represent stable neurophysiologic periods for each of the

four experimental conditions. Large artifacts were removed after visual inspection and the *rejcont* function. Remaining periods of continuous data were segmented into 3-s epochs. Data epochs with remaining large artifacts were removed *via* a combination of visual inspection and the *rej Kurt*, *rejtrend*, and *eegthresh* functions. For each participant, the remaining epochs from the four periods of interest were submitted to independent component analysis (runica function, infomax, extended). Independent components representing eye blink, lateral eye, muscle, facial electromyography, focal channel noise, and focal trial noise were removed from all epochs using visual inspection and the following component classification plugins: SASICA (semi-automated selection of independent components of the electroencephalogram for artifact correction),²³ IC-MARC (independent components of electroencephalogram into multiple artifact classes),²⁴ and ADJUST (automatic electroencephalogram artifact detection based on the joint use of spatial and temporal features).²⁵ All remaining epochs for each period and each participant were then visually inspected again to remove any remaining epochs with excessive artifacts. For the four conditions (baseline, subanesthetic, anesthetic, and recovery), the mean remaining trial counts were 54 (SD = 17), 574 (SD = 48), 66 (SD = 8), and 73 (SD = 11), respectively. The previously removed channels in each data set were interpolated to the 98-channel subset. Spectral power was computed with multitaper spectral analyses (*mtspecgram* function; time window: 3 s, overlap: 0.5 s, number of tapers: 3, time-bandwidth product: 5, spectral resolution: 0.25 Hz). The median absolute power ($10 \cdot \log_{10}[\mu V^2/Hz]$) was calculated for each of the four experimental periods at each of five frequency bands (delta: 1 to 4 Hz, theta: 4 to 8 Hz, alpha: 8 to 13 Hz, beta: 13 to 30 Hz, gamma: 30 to 48 Hz) for all 98 channels and then for eight frontal channels centered on the Fz site (figure in Supplemental Digital Content 1, <http://links.lww.com/ALN/B458>). The final data presented in the spectrograms are the sequential, 3-s epochs (grand-averaged across all participants) that remained after the data-cleaning steps described above were implemented. The data were temporally sequential but not necessarily contiguous given that some epochs were removed after cleaning and artifact removal. Images presented are log-transformed ($10 \cdot \log_{10}$ transform of the grand average of the single-subject data). The recovery period data for one participant were unavailable, and therefore recovery period calculations were completed for only nine participants.

Topographic Analysis. The topographic maps of spectral power for each experimental condition and electroencephalogram bandwidth were constructed using the *topoplot* function in the MATLAB (MathWorks) toolbox EEGLAB.²⁶

Connectivity Processing and Analysis. The selected continuous data epochs from the spectral analyses were used for connectivity analysis without channel interpolation or independent component analysis; this was done to preserve the phase information of the original signals.^{27,28} Additionally, eight occipital channels were removed due to excessive artifact presence, which was deemed necessary for connectivity

analyses, leaving 90 remaining channels. The functional connectivity between electroencephalogram channels was examined across all experimental conditions. The undirected and directed connectivity were measured with debiased weighted phase lag index (wPLI)²⁹ and directed phase lag index (dPLI),³⁰ respectively. The wPLI is a measure of how the instantaneous phases of two electroencephalogram signals are phase-locked to each other. If the instantaneous phase of one signal is consistently ahead or behind of the other signal, the phases are considered locked, and wPLI = 1. However, if the signals randomly alternate between a phase lead and a phase lag relationship, there is no phase locking, and wPLI = 0. The directionality of functional connectivity between two electroencephalogram signals was determined with the asymmetry of the phase lead/lag relationship. If the instantaneous phase of one signal consistently leads that of the other signal, dPLI = 1, and with the inverse case, dPLI = -1. If there is no bias in the phase lead/lag relationship, then dPLI = 0. In practice, both measures are robust to the volume conduction problem of scalp electroencephalography. Electroencephalogram signals were divided into 1-min-long epochs with 50% overlap, which was further divided into 2-s nonoverlapping subepochs. For each subepoch, the cross-spectral density was estimated using the multitaper method, with time-bandwidth product = 2 and the number of tapers = 3,^{21,22} and from these repetitions the averaged wPLI and dPLI values at variable frequencies were estimated using a custom-written function adapted from the Fieldtrip toolbox.³¹ To remove the bias of the measures for a given electroencephalogram data set, the shuffled-data method was used. A series (N = 20) of shuffled signal pairs were generated for each pair of electroencephalogram signals, and the wPLI and dPLI measures were calculated with the shuffled data, the mean of which was subtracted from the raw wPLI and dPLI values as the final estimation of undirected and directed connectivity.³² Final baseline and recovery time epochs were chosen as 2-min segments selected in the middle of each respective recording. Subanesthetic epochs were selected as two sequential 2-min epochs (noted in the figures as Subanes-1 and Subanes-2) that were representative of the observed spectral power during the subanesthetic infusion period. Anesthetic epochs (noted in the figures as Anes-1 and Anes-2) were chosen and displayed in the same manner.

Statistical Analysis

We tested for differences between the experimental periods (baseline, subanesthetic, anesthetic, and recovery) by entering the single-subject electroencephalogram-derived values into a linear-mixed model analysis in SPSS 22 (IBM, USA). Linear-mixed model analysis allowed for statistical comparisons in the event of partially missing data from a given participant (as was the case with missing recovery period data from one volunteer, noted above). Each experimental period served as the fixed factor with participant data serving as a correlated

random effect. We used restricted maximum likelihood estimation and diagonal covariance structure with heterogeneous variances and zero correlation between elements. Direct pairwise comparisons were adjusted using Bonferroni's method. We did not model repeated covariance effects, and a *P* value less than 0.05 was considered statistically significant. The average of median connectivity values was reported for connectivity data, as has been previously described methodologically.⁷ All variability estimates are in SD.

Results

All study participants successfully completed subanesthetic and anesthetic dosing protocols; 6 of 10 (60%) experienced nausea and vomiting after ketamine anesthesia, and 5 of 10 (50%) required additional antiemetic treatment. One volunteer (1 of 10, 10%) briefly required a chin lift and jaw thrust to maintain airway patency shortly after LOC. No adverse clinical events were otherwise noted. All 10 participants experienced LOC after the 1.5 mg/kg ketamine bolus; the mean time between bolus administration and LOC was 1.23 (\pm 0.35) min, and LOC lasted an average of 10.68 (\pm 3.51) min.

Dose-dependent Global Effects of Ketamine—Spectral and Topographic Analysis

Prominent changes were apparent across theta, alpha, and gamma bandwidths. There was a marked increase in theta power during ketamine anesthesia (figs. 1 and 2, and Supplemental Digital Content 2, <http://links.lww.com/ALN/B459>, for individual participants), and this power localized to both frontal and posterior channels (fig. 2). There was a reduction in posterior alpha power from baseline through anesthetic dosing, and no increase or anteriorization of alpha power was noted with either ketamine dose (fig. 2). Increased gamma power was also apparent during the anesthetic epoch compared to other states (figs. 1 and 2).

Frontal Channel Cluster—Ketamine-induced Changes across Brain States

Frontal channels are of particular interest given their accessibility and use in the operating room. During the subanesthetic infusion, a gradual dissipation of alpha power was noted compared to baseline (mean power \pm SD, 0.46 ± 0.34 and 0.88 ± 0.80 dB, respectively), and alpha power remained decreased during the periods of ketamine anesthesia (0.49 ± 0.22 dB) and recovery (0.34 ± 0.38 dB); $F(3,26) = 3.679$, $P < 0.05$ (fig. 3, A and B). With anesthetic dosing, there was a significant increase in theta bandwidth power (4.25 ± 1.90 dB) compared to baseline (0.64 ± 0.28 dB), subanesthetic (0.60 ± 0.30 dB), and recovery (0.68 ± 0.41 dB) periods; $F(3,26) = 41.01$, $P < 0.001$ (fig. 3, A and B; table 1). Theta power was not otherwise significantly modulated during nonanesthetic periods, and relative increases in theta power during ketamine anesthesia were higher than that of any other bandwidth (table 1).

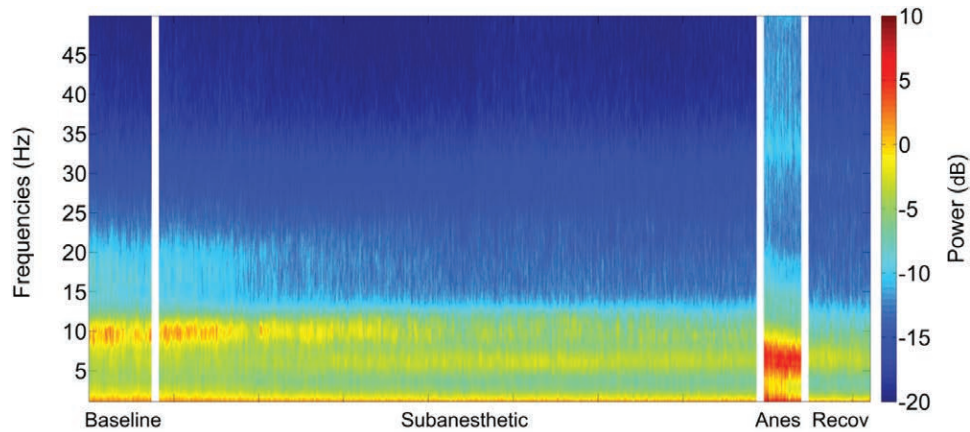


Fig. 1. Group-level absolute power spectrogram (0.05- to 55-Hz bandpass filter). There is a marked increase in theta bandwidth power during ketamine anesthesia. Anes = anesthetic period; Recov = recovery period.

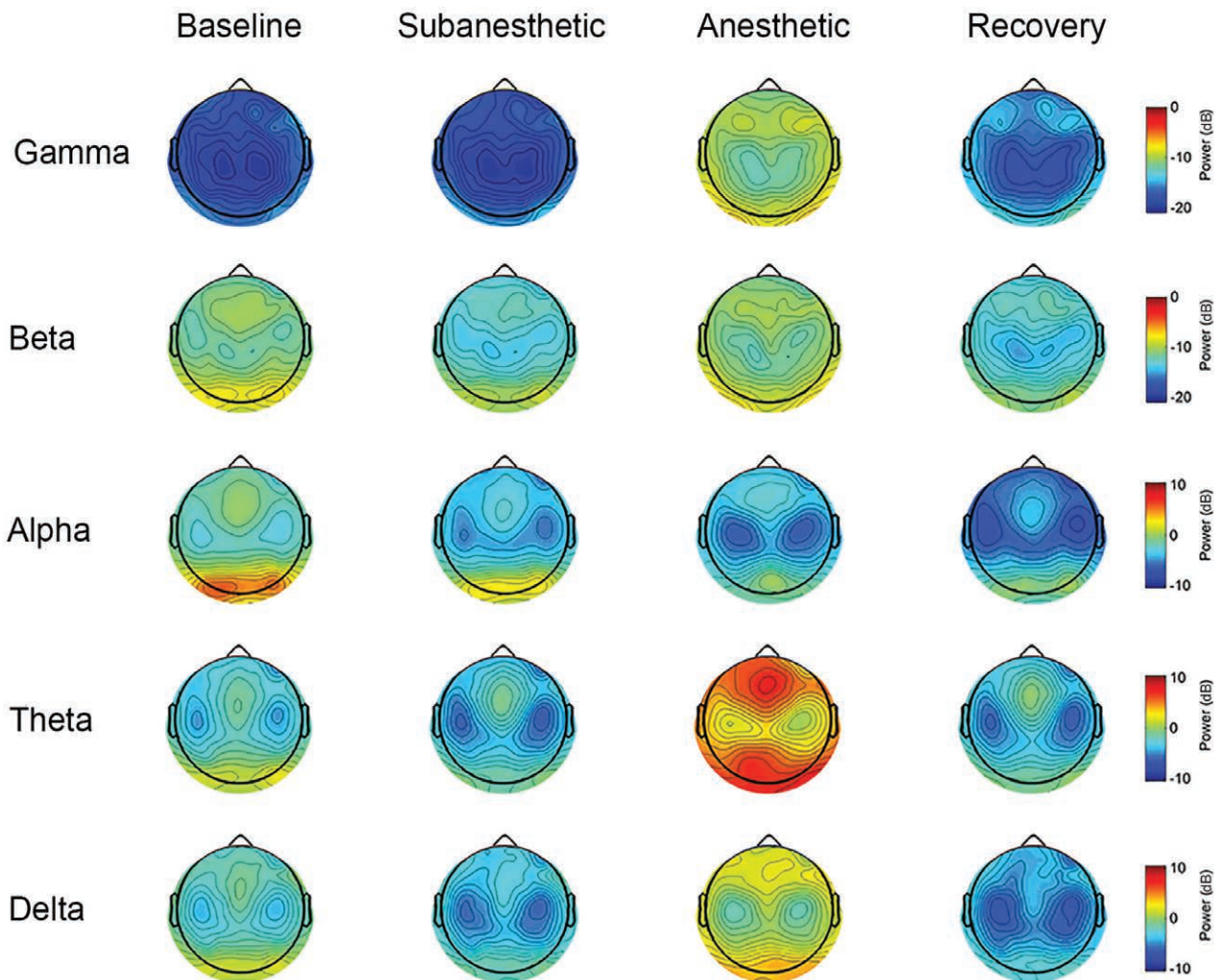


Fig. 2. Topomaps from retained trials for each condition. During ketamine anesthesia, theta power increases in frontal and posterior channel clusters. Posterior alpha power decreases sequentially during subanesthetic and anesthetic ketamine dosing, and no anteriorization of alpha power is noted during anesthetic dosing (delta, 1 to 4 Hz; theta, 4 to 8 Hz; alpha, 8 to 13 Hz; beta, 13 to 30 Hz; and gamma, 30 to 48 Hz).

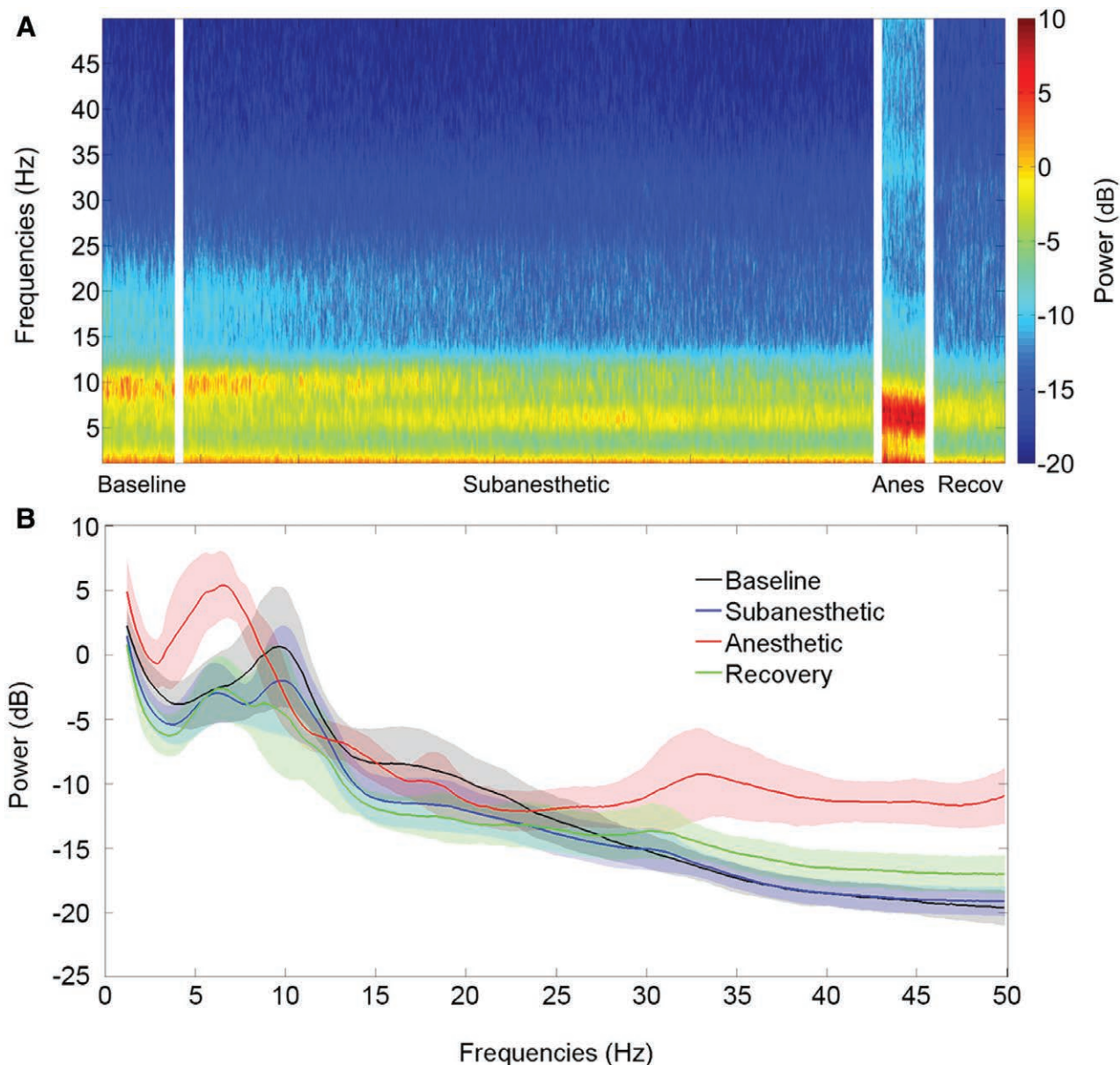


Fig. 3. Frontal channel, group-level spectrogram, and line graph (see figure in Supplemental Digital Content 1, <http://links.lww.com/ALN/B458>, for electrode placement location). (A) Spectrogram depicts marked increase in frontal channel theta power during the anesthetic period. Increased gamma bandwidth power compared to baseline is noted as well. (B) Line graph demonstrates a shift to theta bandwidth power during ketamine anesthesia. Shaded regions represent ± 1 SD. Anes = anesthetic period; Recov = recovery period.

Functional Connectivity Analyses

Given the significant increases in theta power and decreases in alpha power with progressive ketamine dosing, we undertook connectivity analyses in these bandwidths across each condition. Reduced functional connectivity in the alpha bandwidth has also been previously demonstrated with anesthetic ketamine dosing,¹¹ further motivating our choice of bandwidths for analysis. Although we noted marked increases in gamma bandwidth power, electromyographic artifact might contribute to gamma activity despite our data cleaning.^{33,34} Thus, we did not examine gamma connectivity

in this study. Furthermore, subanesthetic ketamine has been shown to increase gamma power in other paradigms,^{35,36} whereas increased theta power seems to correlate specifically to the anesthetized state.^{19,37,38}

Weighted Phase Lag Index—Theta Phase Locking during Ketamine Anesthesia

Figure 4 presents the global and regional wPLI changes across each experimental condition. Figure 4A shows the average median wPLI between anterior and posterior regions in the time and frequency domains (see Supplemental Digital

Table 1. Mean Power Values across Ketamine Doses and Electroencephalogram Bandwidths—Frontal Channels

Bandwidth	Mean Power \pm SD, dB			
	Baseline	Subanesthetic Dose	Anesthetic Dose	Recovery
Gamma (> 30 Hz)	0.02 \pm 0.00	0.02 \pm 0.00	0.09 \pm 0.06	0.03 \pm 0.01
Beta (13–30 Hz)	0.09 \pm 0.04	0.06 \pm 0.02	0.08 \pm 0.03	0.06 \pm 0.02
Alpha (8–13 Hz)	0.88 \pm 0.80	0.46 \pm 0.34	0.49 \pm 0.22	0.34 \pm 0.38
Theta (4–8 Hz)	0.64 \pm 0.28	0.60 \pm 0.30	4.25 \pm 1.90	0.68 \pm 0.41
Delta (1–4 Hz)	0.72 \pm 0.23	0.46 \pm 0.13	1.39 \pm 0.70	0.36 \pm 0.12

Absolute power values across conditions and frequency bandwidths in frontal channels are shown. Linear-mixed modeling analysis was used for statistical comparisons; $P < 0.001$ for all bandwidths except alpha ($P < 0.05$).

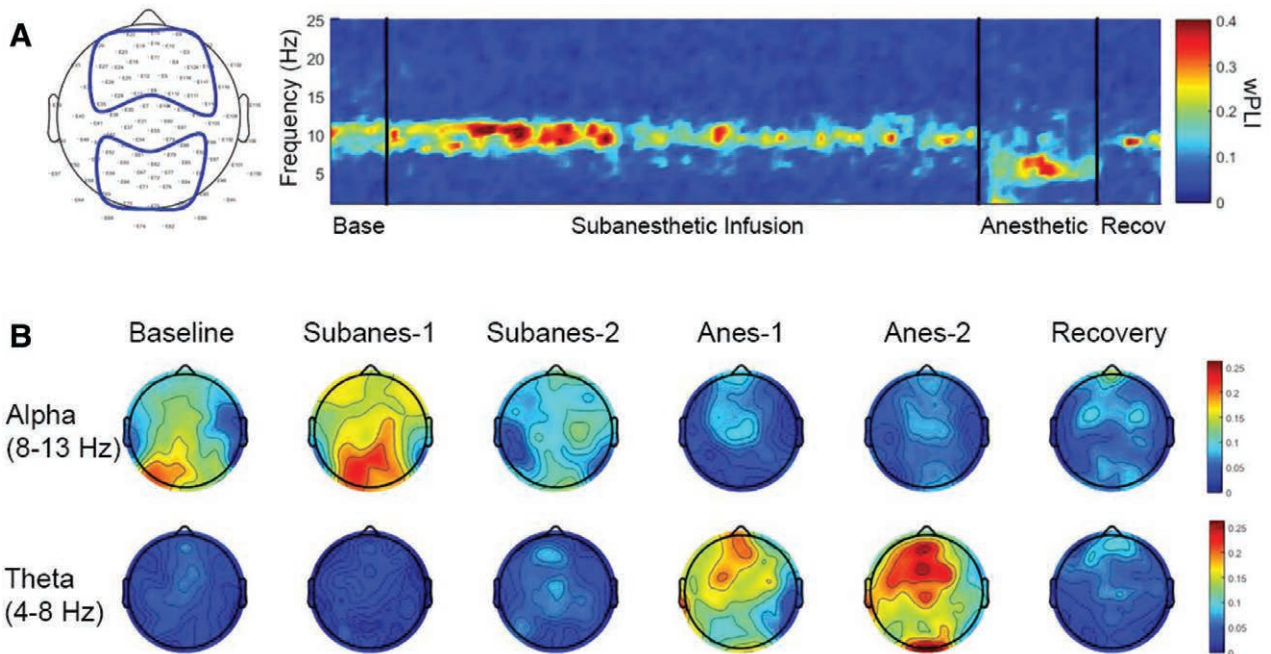


Fig. 4. Weighted functional connectivity changes, as assessed by weighted phase lag index (wPLI). (A) Group level connectogram of the mean wPLI between anterior and posterior regions. The vertical black lines separate the baseline, subanesthetic, anesthetic, and recovery periods. The time periods during subanesthetic and anesthetic recordings were rescaled; the horizontal axis indicates number of epochs (1-min long with 50% overlapping). (B) Scalp topography of the mean wPLI at alpha (8 to 13 Hz) and theta (4 to 8 Hz) for the six periods studied. Anes-1 = first anesthetic period examined; Anes-2 = second anesthetic period examined; Base = baseline period; Recov = recovery period; Subanes-1 = first subanesthetic period examined; Subanes-2 = second subanesthetic period examined.

Content 3, <http://links.lww.com/ALN/B460>, for individual participants). Alpha wPLI was dominant at baseline and increased during the initial phase of the subanesthetic infusion (fig. 4A). During the anesthetic period, however, wPLI connectivity strength shifted to the theta bandwidth (fig. 4A). Figure 4B presents the topographic changes of global wPLI networks for the theta and alpha bandwidths across experimental conditions. Within the anterior region, theta wPLI was highest during the anesthetic period (mean wPLI \pm SD; 0.2349 \pm 0.1170) compared to all other states; $F(5,44) = 7.996$, $P < 0.001$ (fig. 3B). Theta wPLI was also highest during ketamine anesthesia between anterior and posterior regions (0.2159 \pm 0.1538); $F(5,44) = 4.192$, $P < 0.01$ (fig. 3B). Alpha wPLI within the anterior region

remained relatively unchanged throughout each study condition, $F(5,44) = 0.697$, $P = 0.628$, although significant changes were noted between anterior and posterior regions, with mean wPLI lowest (0.0833 \pm 0.1083) during the anesthetic period; $F(5,44) = 3.147$, $P < 0.05$ (fig. 4B).

Directed Phase Lag Index—Directional Connectivity Changes during Ketamine Anesthesia

Figure 5 demonstrates how the directionality of functional connectivity changed across the experimental conditions. Figure 5A shows the average median dPLI between anterior and posterior electrodes in the time and frequency domains (see Supplemental Digital Content 3, <http://links.lww.com/ALN/B460>, for individual participants). An anterior-to-posterior directionality

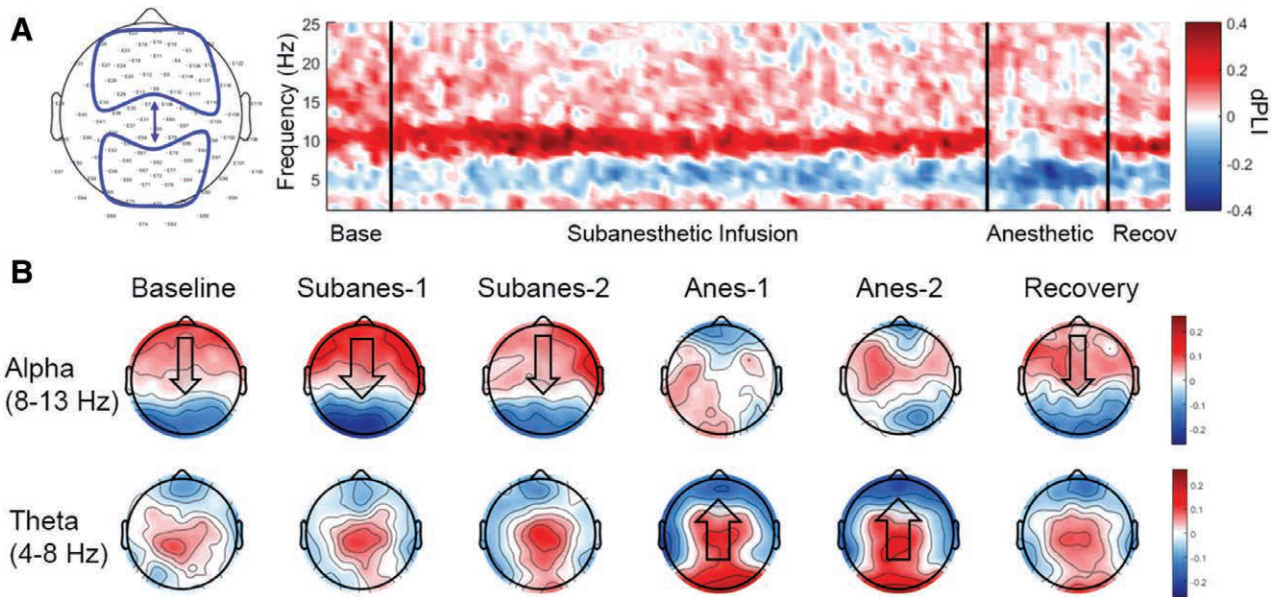


Fig. 5. Directional functional connectivity changes, as assessed by directed phase lag index (dPLI), across all conditions in the alpha and theta bandwidths. (A) Group-level connectogram of the mean dPLI between anterior and posterior regions. The vertical black lines separate the baseline (Base), subanesthetic, anesthetic, and recovery periods. Time on the horizontal axis was rescaled; epochs are 1-min long with 50% overlap. (B) Scalp topograph of the mean dPLI (in each channel and with all other channels) at alpha and theta for the six studied conditions. Anes-1 = first anesthetic period examined; Anes-2 = second anesthetic period examined; Recov = recovery period; Subanes-1 = first subanesthetic period examined; Subanes-2 = second subanesthetic period examined.

(the positive dPLIs denoted with red color) was observed in the alpha bandwidth during the baseline and subanesthetic periods. Theta shows a consistently opposite directionality from posterior-to-anterior regions (the negative dPLI denoted with blue color). Figure 5B shows the frequency-specific and state-specific topographies of electroencephalographic directionality. Alpha dPLI was maximally reduced between anterior and posterior channels during ketamine anesthesia (mean dPLI \pm SD, 0.0282 ± 0.0772 ; $F(5,44) = 2.484$; $P < 0.05$ (fig. 4B). Alpha dPLI was also examined between prefrontal and frontal channels and was again maximally reduced during ketamine anesthesia (-0.0224 ± 0.0400 ; $F(5,44) = 4.137$; $P < 0.01$ (fig. 4B). Compared to baseline (0.0427 ± 0.0717), direct pairwise comparisons (with Bonferroni correction) revealed a statistically significant reduction in alpha dPLI only during each of the anesthetic epochs (Anes-1, -0.0170 ± 0.0481 , $P < 0.05$; Anes-2, -0.0224 ± 0.0400 , $P < 0.05$). Thus, an overall maximally reduced anterior-to-posterior connectivity pattern was demonstrated with alpha dPLI during ketamine anesthesia among these channel regions. Although a posterior-to-anterior pattern was noted with theta dPLI during ketamine anesthesia (fig. 5B), these associations did not reach statistically significant differences between anterior and posterior channels, $F(5,44) = 0.177$, $P = 0.970$, or for prefrontal and frontal channels, $F(5, 44) = 0.768$, $P = 0.578$.

Discussion

This study characterized ketamine-induced electroencephalographic changes during subanesthetic, anesthetic, and recovery

periods (relative to baseline) in healthy volunteers using high-density electroencephalography. During subanesthetic ketamine administration, spectral power gradually (and modestly) shifts from the alpha bandwidth to the theta bandwidth, with anterior-to-posterior connectivity (as measured by alpha dPLI) maintained. During ketamine anesthesia, however, the power shifts dramatically to the theta bandwidth, theta wPLI increases in anterior and posterior regions, and anterior-to-posterior alpha connectivity (as measured by alpha dPLI) is significantly reduced. Upon recovery, these connectivity patterns return to near-baseline levels in each bandwidth. Ketamine anesthesia was also associated with increased gamma and delta power, as previously reported,^{10,12,13} and frontal gamma power remained slightly elevated compared to baseline.

Our results demonstrate increased theta power correlating with ketamine anesthesia. Of note, increased theta oscillatory activity during ketamine anesthesia was first documented more than five decades ago. In the seminal human study that first examined the pharmacologic effects of ketamine in 1965, Domino *et al.*³⁷ remarked, "Characteristic thetalike waves were recorded at dosage levels which produced coma; these were distributed over most of the cerebral hemisphere." Increased theta activity has since been documented during anesthetic ketamine administration.^{13,15,38} A strictly receptor- and channel-based explanation for this theta resonance may be difficult to describe, because ketamine has a considerably diverse array of molecular targets.^{1,2,5,6,39–42} A network-level consideration of the phenomenon might provide insight regarding the consequences for information processing. In the

awake state, theta and alpha frequencies interact in a circular, reciprocating pattern of “information flow” between anterior and posterior brain regions.^{43,44} Although oscillatory amplitude and phase are theoretically independent, amplitude (and thus power) may associate with phase to facilitate interactions with other neuronal populations within a network.⁴⁵ As alpha power and anterior-to-posterior connectivity become maximally depressed during ketamine anesthesia, increased theta power and phase locking between the anterior and posterior regions may represent large-scale network disequilibrium. This is, however, a speculative interpretation, and additional studies are needed to further explore the neurobiologic relevance of such connectivity patterns. From a clinical perspective, the distinct appearance of theta power during anesthesia may be informative for clinicians who routinely administer ketamine. The appearance of increasing theta power could alert clinicians to anesthetic ketamine dosing, which may be particularly helpful in settings where subanesthetic dosing is desired (as in the treatment of depression).^{46,47} As the global and frontal spectrograms in this study both illustrated marked increases in theta power during ketamine anesthesia, the use of frontal electroencephalogram channels alone may be sufficient to monitor for this theta signature.

It is notable that ketamine anesthesia is associated with a maximal depression of anterior-to-posterior connectivity in the alpha bandwidth. Inhibition of frontal-to-parietal connectivity (with certain measures) has correlated with general anesthesia in humans across a diverse range of anesthetics,^{12,32,48,49} and our group has previously demonstrated reduced alpha directional connectivity during ketamine anesthesia with low-resolution electroencephalography.¹¹ Recently, disruptions in NMDA- and α -amino-3-hydroxy-5-methyl-4-isoxazolepropionic acid-mediated frontoparietal connectivity patterns have been demonstrated during subanesthetic ketamine administration in healthy volunteers,³⁵ who remained conscious during these experiments. This raises the possibility that disrupted frontal-to-parietal connectivity may not strictly correlate with anesthetic-induced unconsciousness. An alternative explanation, however, is that such connectivity

was not maximally depressed during these subanesthetic infusion periods. Findings from our study demonstrate that alpha directional connectivity remained relatively unchanged during subanesthetic dosing, decreased dramatically during anesthetic ketamine administration, and returned to baseline levels at recovery. The connectograms (figs. 4A and 5A) demonstrate significant functional connectivity in the alpha bandwidth during baseline and subanesthetic states—despite a gradual reduction of power—and this connectivity diminishes significantly during ketamine anesthesia. Thus, there may be a dose-dependent relationship between connectivity and loss of consciousness. In fact, Untergerher *et al.*⁵⁰ illustrated dynamic fluctuations in functional connectivity patterns, whereby maximum functional connectivity occurs during varying time intervals on a continuous scale, with surrogates of information transfer times being fastest during unconsciousness. Accordingly, connectivity is a dynamic process and may need to cross certain real-time, continuous thresholds to correlate with varying levels of consciousness.

Multiple and unique strengths of this study are worth highlighting. No other sedative, opioid, or hypnotic medications were administered; thus, electroencephalographic effects of ketamine were not confounded by coadministration of other psychoactive medications. Additionally, an advanced-data cleaning process was used for spectral analysis. In addition to visual inspection, data from each time epoch underwent independent component analysis blind-source separation, and independent components representing eye blink, eye muscle, facial muscle, channel noise, and single-trial artifact were removed. Analytic comparisons were also made across multiple states—we were able to compare effects of ketamine before administration, at both subanesthetic and anesthetic doses, and during recovery. High-density electroencephalography was utilized, allowing for high-resolution and multiregional analyses. Last, functional connectivity based on phase relationships was also assessed with the use of wPLI and dPLI. To our knowledge, this is the first study to combine all of these methodologic strengths for the electroencephalographic analysis of ketamine in humans (table 2).

Table 2. Related Human Studies Examining the Effects of Ketamine on Electroencephalographic and Magnetoencephalographic Recordings

Study	High-density Data Acquisition	Subanesthetic Dosing	Anesthetic Dosing	Recovery Period	Ketamine Only	Connectivity/Coherence Analysis
Domino <i>et al.</i> , 1965 ³⁷		*	*	*	*	
Schüttler <i>et al.</i> , 1987 ³⁸		*	*	*	*	
Kochs <i>et al.</i> , 1996 ¹⁹		*	*	*	*	
Lee <i>et al.</i> , 2013 ¹²			*		*	*
Blain-Moraes <i>et al.</i> , 2014 ¹¹			*		*	*
Muthukumaraswamy <i>et al.</i> , 2015 ³⁵	*	*		*	*	*
Rivolta <i>et al.</i> , 2015 ³⁶	*	*			*	*
Akeju <i>et al.</i> , 2016 ¹³			*			*
Vlisides <i>et al.</i> , 2017 (current article)	*	*	*	*	*	*

*Presence of the specified methodologic consideration for each given study.

There are significant limitations to the study as well. Administering the subanesthetic ketamine infusion immediately before anesthetic dosing may influence neurophysiologic patterns observed during the anesthetic period. Our spectral data demonstrate a gradual reduction in alpha bandwidth power and increased theta power during the subanesthetic infusion. Whether this preceding subanesthetic exposure modulates subsequent neurophysiology and network connectivity during anesthetic dosing is unclear. Additionally, although a 128-channel electroencephalogram system was used, 86 to 91 channels were ultimately retained for spectral analyses after removal of artifact and bad channels. These artifact-removal strategies may also yield spectral patterns that differ from a real-world, clinical setting. For example, ocular artifact removal may have attenuated changes in delta power that might otherwise be present.⁵¹ As we wanted to optimize electroencephalogram data for connectivity analyses, we did not employ the same artifact-removal strategies (*e.g.*, independent component analysis) as the spectral analyses, because they may interfere with phase-synchronization data.^{27,28} Thus, spectral and connectivity data results emerged from different data-processing steps. The administration of both ondansetron and scopolamine could potentially have modulated central neurophysiology, but we regarded this as unlikely, and both of these medications were ultimately warranted for participant comfort. Participants were instructed to keep their eyes closed during each experimental period, but sporadic eye opening was noted throughout the recording sessions. This could have impacted certain epochs of the neurophysiologic data acquisition and analysis.

There are also significant limitations to consider regarding connectivity analyses. Although connectivity measures (in this case, wPLI and dPLI) are used as surrogates for functional interactions across the cortex, this is merely an assumption. Our recent data in nonhuman primates confirm a breakdown of corticocortical information transfer during ketamine anesthesia,⁵² but different connectivity measures or experimental conditions can yield disparate results.⁴³ The phase lag index can also be associated with significant inter-subject variability, particularly given the complex neural processes associated with these phase-based methods; as a result, phase lag index is often not amenable to statistical averaging or traditional artifact reduction strategies.⁵³ In terms of the general interpretation of directional connectivity results, it must be kept in mind that these measures reflect a large spatial scale and a long temporal scale, with an unclear relationship to the underlying neural spiking networks. As an intuitive example, the Dow Jones Industrial Average samples the performance of only a select number of publically traded companies. As a single value that rises or falls, it does not capture the rich dynamics and widespread stock exchange on the trading-room floor. Similarly, directed connectivity measures sample features that might reflect large-scale cortical interactions, but they do not capture the neuronal dynamics and widespread information exchange in cortical and subcortical

systems. With that being said, changes in directed connectivity measures and surrogates of information transfer observed in the brain during anesthetic-induced unconsciousness have been shown to reflect fundamental network properties.⁴⁵

In summary, this study used high-resolution electroencephalographic data to characterize ketamine-induced changes across multiple doses and associated levels of consciousness. Notably, increased theta power and phase locking occur between anterior and posterior regions during ketamine anesthesia, returning to baseline upon recovery. Anterior-to-posterior connectivity in the alpha bandwidth was maximally suppressed during ketamine anesthesia, and this connectivity is also restored to baseline levels during recovery. This constellation of power and connectivity results (increased theta power, as seen during rapid-eye-movement sleep, coupled with loss of anterior-to-posterior alpha connectivity, as seen during anesthesia) might contribute to the unique qualities of ketamine anesthesia.

Acknowledgments

The authors thank Yumeng Li, M.S., Center for Statistical Consultation and Research, University of Michigan, Ann Arbor, Michigan, for statistical consultation.

Research Support

Supported by grant Nos. T32GM103730 (to Drs. Vlisides and Mashour) and R01GM111293 (to Dr. Mashour) from the National Institutes of Health, Bethesda, Maryland, and by the Department of Anesthesiology, University of Michigan, Ann Arbor, Michigan.

Competing Interests

The authors declare no competing interests.

Correspondence

Address correspondence to Dr. Mashour: Department of Anesthesiology, Center for Consciousness Science, University of Michigan Medical School, 1H247 UH, SPC-5048, 1500 East Medical Center Drive, Ann Arbor, Michigan 48109-5048. gmashour@med.umich.edu. Information on purchasing reprints may be found at www.anesthesiology.org or on the masthead page at the beginning of this issue. ANESTHESIOLOGY's articles are made freely accessible to all readers, for personal use only, 6 months from the cover date of the issue.

References

1. Anis NA, Berry SC, Burton NR, Lodge D: The dissociative anaesthetics, ketamine and phencyclidine, selectively reduce excitation of central mammalian neurones by *N*-methylaspartate. *Br J Pharmacol* 1983; 79:565–75
2. Thomson AM, West DC, Lodge D: An *N*-methylaspartate receptor-mediated synapse in rat cerebral cortex: A site of action of ketamine? *Nature* 1985; 313:479–81
3. Yamamura T, Harada K, Okamura A, Kemmotsu O: Is the site of action of ketamine anesthesia the *N*-methyl-D-aspartate receptor? *ANESTHESIOLOGY* 1990; 72:704–10
4. Petrenko AB, Yamakura T, Fujiwara N, Askalany AR, Baba H, Sakimura K: Reduced sensitivity to ketamine and pentobarbital in mice lacking the *N*-methyl-D-aspartate receptor

- GluRepsilon1 subunit. *Anesth Analg* 2004; 99:1136–40, table of contents
5. Chen X, Shu S, Bayliss DA: HCN1 channel subunits are a molecular substrate for hypnotic actions of ketamine. *J Neurosci* 2009; 29:600–9
 6. Zhou C, Douglas JE, Kumar NN, Shu S, Bayliss DA, Chen X: Forebrain HCN1 channels contribute to hypnotic actions of ketamine. *ANESTHESIOLOGY* 2013; 118:785–95
 7. Purdon PL, Pierce ET, Mukamel EA, Prerau MJ, Walsh JL, Wong KF, Salazar-Gomez AF, Harrell PG, Sampson AL, Cimenser A, Ching S, Kopell NJ, Tavares-Stoekel C, Habeeb K, Merhar R, Brown EN: Electroencephalogram signatures of loss and recovery of consciousness from propofol. *Proc Natl Acad Sci USA* 2013; 110:E1142–51
 8. Lewis LD, Weiner VS, Mukamel EA, Donoghue JA, Eskandar EN, Madsen JR, Anderson WS, Hochberg LR, Cash SS, Brown EN, Purdon PL: Rapid fragmentation of neuronal networks at the onset of propofol-induced unconsciousness. *Proc Natl Acad Sci USA* 2012; 109:E3377–86
 9. Vijayan S, Ching S, Purdon PL, Brown EN, Kopell NJ: Thalamocortical mechanisms for the anteriorization of α rhythms during propofol-induced unconsciousness. *J Neurosci* 2013; 33:11070–5
 10. Purdon PL, Sampson A, Pavone KJ, Brown EN: Clinical electroencephalography for anesthesiologists: Part I. Background and basic signatures. *ANESTHESIOLOGY* 2015; 123:937–60
 11. Blain-Moraes S, Lee U, Ku S, Noh G, Mashour GA: Electroencephalographic effects of ketamine on power, cross-frequency coupling, and connectivity in the alpha bandwidth. *Front Syst Neurosci* 2014; 8:114
 12. Lee U, Ku S, Noh G, Baek S, Choi B, Mashour GA: Disruption of frontal-parietal communication by ketamine, propofol, and sevoflurane. *ANESTHESIOLOGY* 2013; 118:1264–75
 13. Akeju O, Song AH, Hamilos AE, Pavone KJ, Flores FJ, Brown EN, Purdon PL: Electroencephalogram signatures of ketamine anesthesia-induced unconsciousness. *Clin Neurophysiol* 2016; 127:2414–22
 14. Tsuda N, Hayashi K, Hagihira S, Sawa T: Ketamine, an NMDA-antagonist, increases the oscillatory frequencies of alpha-peaks on the electroencephalographic power spectrum. *Acta Anaesthesiol Scand* 2007; 51:472–81
 15. Bojak I, Day HC, Liley DT: Ketamine, propofol, and the EEG: A neural field analysis of HCN1-mediated interactions. *Front Comput Neurosci* 2013; 7:22
 16. Olney JW, Newcomer JW, Farber NB: NMDA receptor hypofunction model of schizophrenia. *J Psychiatr Res* 1999; 33:523–33
 17. Kurehara K, Asano N, Iwata T, Yamaguchi A, Kawano Y, Furuya H: [The influence of ketamine on the bispectral index, the spectral edge frequency 90 and the frequency bands power during propofol anesthesia] (translated from Japanese). *Masui* 1999; 48:611–6
 18. Shaw AD, Saxena N, E Jackson L, Hall JE, Singh KD, Muthukumaraswamy SD: Ketamine amplifies induced gamma frequency oscillations in the human cerebral cortex. *Eur Neuropsychopharmacol* 2015; 25:1136–46
 19. Kochs E, Scharein E, Möllenberg O, Bromm B, Schulte am Esch J: Analgesic efficacy of low-dose ketamine: Somatosensory-evoked responses in relation to subjective pain ratings. *ANESTHESIOLOGY* 1996; 85:304–14
 20. Blain-Moraes S, Tarnal V, Vanini G, Alexander A, Rosen D, Shortal B, Janke E, Mashour GA: Neurophysiological correlates of sevoflurane-induced unconsciousness. *ANESTHESIOLOGY* 2015; 122:307–16
 21. Bokil H, Andrews P, Kulkarni JE, Mehta S, Mitra PP: Chronux: A platform for analyzing neural signals. *J Neurosci Methods* 2010; 192:146–51
 22. Mitra PP, Bokil H: *Observed Brain Dynamics*. New York, Oxford University Press, 2008
 23. Chaumon M, Bishop DV, Busch NA: A practical guide to the selection of independent components of the electroencephalogram for artifact correction. *J Neurosci Methods* 2015; 250:47–63
 24. Frølich L, Andersen TS, Mørup M: Classification of independent components of EEG into multiple artifact classes. *Psychophysiology* 2015; 52:32–45
 25. Mognon A, Jovicich J, Bruzzone L, Buiatti M: ADJUST: An automatic EEG artifact detector based on the joint use of spatial and temporal features. *Psychophysiology* 2011; 48:229–40
 26. Delorme A, Makeig S: EEGLAB: An open source toolbox for analysis of single-trial EEG dynamics including independent component analysis. *J Neurosci Methods* 2004; 134:9–21
 27. Meinecke FC, Ziehe A, Kurths J, Müller KR: Measuring phase synchronization of superimposed signals. *Phys Rev Lett* 2005; 94:084102
 28. Nolte G, Meinecke FC, Ziehe A, Müller KR: Identifying interactions in mixed and noisy complex systems. *Phys Rev E Stat Nonlin Soft Matter Phys* 2006; 73:051913
 29. Vinck M, Oostenveld R, van Wingerden M, Battaglia F, Pennartz CM: An improved index of phase-synchronization for electrophysiological data in the presence of volume-conduction, noise and sample-size bias. *Neuroimage* 2011; 55:1548–65
 30. Stam CJ, van Straaten EC: Go with the flow: Use of a directed phase lag index (dPLI) to characterize patterns of phase relations in a large-scale model of brain dynamics. *Neuroimage* 2012; 62:1415–28
 31. Oostenveld R, Fries P, Maris E, Schoffelen JM: FieldTrip: Open source software for advanced analysis of MEG, EEG, and invasive electrophysiological data. *Comput Intell Neurosci* 2011; 2011:156869
 32. Papan A, Kugiumtzis D, Larsson PG: Reducing the bias of causality measures. *Phys Rev E Stat Nonlin Soft Matter Phys* 2011; 83:036207
 33. Whitham EM, Pope KJ, Fitzgibbon SP, Lewis T, Clark CR, Loveless S, Broberg M, Wallace A, DeLosAngeles D, Lillie P, Hardy A, Fronsco R, Pulbrook A, Willoughby JO: Scalp electrical recording during paralysis: Quantitative evidence that EEG frequencies above 20 Hz are contaminated by EMG. *Clin Neurophysiol* 2007; 118:1877–88
 34. Whitham EM, Lewis T, Pope KJ, Fitzgibbon SP, Clark CR, Loveless S, DeLosAngeles D, Wallace AK, Broberg M, Willoughby JO: Thinking activates EMG in scalp electrical recordings. *Clin Neurophysiol* 2008; 119:1166–75
 35. Muthukumaraswamy SD, Shaw AD, Jackson LE, Hall J, Moran R, Saxena N: Evidence that subanesthetic doses of ketamine cause sustained disruptions of NMDA and AMPA-mediated frontoparietal connectivity in humans. *J Neurosci* 2015; 35:11694–706
 36. Rivolta D, Heidegger T, Scheller B, Sauer A, Schaum M, Birkner K, Singer W, Wibral M, Uhlhaas PJ: Ketamine dysregulates the amplitude and connectivity of high-frequency oscillations in cortical-subcortical networks in humans: Evidence from resting-state magnetoencephalography-recordings. *Schizophr Bull* 2015; 41:1105–14
 37. Domino EF, Chodoff P, Corssen G: Pharmacologic effects of CI-581, a new dissociative anesthetic, in man. *Clin Pharmacol Ther* 1965; 6:279–91
 38. Schüttler J, Stanski DR, White PF, Trevor AJ, Horai Y, Verotta D, Sheiner LB: Pharmacodynamic modeling of the EEG effects of ketamine and its enantiomers in man. *J Pharmacokinetics Biopharm* 1987; 15:241–53
 39. Yamakage M, Hirshman CA, Croxton TL: Inhibitory effects of thiopental, ketamine, and propofol on voltage-dependent Ca^{2+} channels in porcine tracheal smooth muscle cells. *ANESTHESIOLOGY* 1995; 83:1274–82
 40. Hayashi Y, Kawaji K, Sun L, Zhang X, Koyano K, Yokoyama T, Kohsaka S, Inoue K, Nakanishi H: Microglial Ca^{2+} -activated

- K⁺ channels are possible molecular targets for the analgesic effects of S-ketamine on neuropathic pain. *J Neurosci* 2011; 31:17370–82
41. Yamakura T, Chavez-Noriega LE, Harris RA: Subunit-dependent inhibition of human neuronal nicotinic acetylcholine receptors and other ligand-gated ion channels by dissociative anesthetics ketamine and dizocilpine. *ANESTHESIOLOGY* 2000; 92:1144–53
 42. Cai YC, Ma L, Fan GH, Zhao J, Jiang LZ, Pei G: Activation of *N*-methyl-D-aspartate receptor attenuates acute responsiveness of delta-opioid receptors. *Mol Pharmacol* 1997; 51:583–7
 43. Hillebrand A, Tewarie P, van Dellen E, Yu M, Carbo EW, Douw L, Gouw AA, van Straaten EC, Stam CJ: Direction of information flow in large-scale resting-state networks is frequency-dependent. *Proc Natl Acad Sci USA* 2016; 113:3867–72
 44. Meier J, Zhou X, Hillebrand A, Tewarie P, Stam CJ, Van Mieghem P: The epidemic spreading model and the direction of information flow in brain networks. *Neuroimage* 2017; 152:639–46
 45. Moon JY, Lee U, Blain-Moraes S, Mashour GA: General relationship of global topology, local dynamics, and directionality in large-scale brain networks. *PLoS Comput Biol* 2015; 11:e1004225
 46. Singh JB, Fedgchin M, Daly EJ, De Boer P, Cooper K, Lim P, Pinter C, Murrrough JW, Sanacora G, Shelton RC, Kurian B, Winokur A, Fava M, Manji H, Drevets WC, Van Nueten L: A double-blind, randomized, placebo-controlled, dose-frequency study of intravenous ketamine in patients with treatment-resistant depression. *Am J Psychiatry* 2016; 173:816–26
 47. Newton A, Fitton L: Intravenous ketamine for adult procedural sedation in the emergency department: A prospective cohort study. *Emerg Med J* 2008; 25:498–501
 48. Imas OA, Ropella KM, Ward BD, Wood JD, Hudetz AG: Volatile anesthetics disrupt frontal-posterior recurrent information transfer at gamma frequencies in rat. *Neurosci Lett* 2005; 387:145–50
 49. Boly M, Moran R, Murphy M, Boveroux P, Bruno MA, Noirhomme Q, Ledoux D, Bonhomme V, Brichant JF, Tononi G, Laureys S, Friston K: Connectivity changes underlying spectral EEG changes during propofol-induced loss of consciousness. *J Neurosci* 2012; 32:7082–90
 50. Untergehrer G, Jordan D, Kochs EF, Ilg R, Schneider G: Fronto-parietal connectivity is a non-static phenomenon with characteristic changes during unconsciousness. *PLoS One* 2014; 9:e87498
 51. Waterman D, Woestenburg JC, Elton M, Hofman W, Kok A: Removal of ocular artifacts from the REM sleep EEG. *Sleep* 1992; 15:371–5
 52. Schroeder KE, Irwin ZT, Gaidica M, Bentley JN, Patil PG, Mashour GA, Chestek CA: Disruption of corticocortical information transfer during ketamine anesthesia in the primate brain. *Neuroimage* 2016; 134:459–65
 53. Lau TM, Gwin JT, McDowell KG, Ferris DP: Weighted phase lag index stability as an artifact resistant measure to detect cognitive EEG activity during locomotion. *J Neuroeng Rehabil* 2012; 9:47